Journal of Catalysis **202,** 256–267 (2001)
doi:10.1006/jcat.2001.3290, available online at http://www.idealibrary.com on IDEAL®

Au/TiO_2 Nanosized Samples: A Catalytic, TEM, and FTIR Study of the Effect of Calcination Temperature on the CO Oxidation

Flora Boccuzzi,*,[1] Anna Chiorino,* Maela Manzoli,* Ping Lu,† Tomoki Akita,† Satoshi Ichikawa,† and Masatake Haruta†

*Dipartimento di Chimica I.F.M., via P. Giuria 7, 10125 Torino, Italy; and †Osaka National Research Institute, AIST, Midorigaoka 1, Ikeda 563, Japan

Received January 16, 2001; revised May 16, 2001; accepted May 21, 2001; published online August 9, 2001

Three Au/TiO_2 catalysts, with the same Au loading and with different particle sizes, were prepared by the deposition–precipitation method followed by calcination at three different temperatures, 473, 573, and 873 K. The mean diameters of Au particles were 2.4, 2.5, and 10.6 nm, respectively. On all the samples the CO adsorption and different CO–O_2 interactions were examined by FTIR at 90 K and at room temperature. The higher catalytic activity on CO oxidation found for the samples calcined at 473 and 573 K is related to the higher concentration of step sites over the Au surfaces and to a higher concentration of step sites at the borderline with the support. At 90 K, CO and molecular oxygen are competitively adsorbed on step sites. By CO preadsorption on hydrated catalysts, the reaction with O_2 gives CO_2 already at 90 K, while by oxygen preadsorption the reaction is completely inhibited, unless moisture is present in the gas phase. An effect of CO coadsorption has been evidenced on water dissociation on gold sites or at the interface with the support, producing atomic hydrogen. The hydrogen reacts with the oxygen, producing a reactive species, quickly dissociated in nascent oxygen and OH groups. Moreover, the reaction with $^{18}O_2$ at 90 K in the presence of moisture produces only $C^{16}O^{18}O$, giving evidence that there is no direct participation of oxygens of the support and of the water in the reaction. At room temperature, other reaction channels become operative, involving oxygen species activated on the support, as shown by the extensive exchange reactions occurring with the support oxygen.

Key Words: **gold catalysts; CO oxidation; size effects; TEM and FTIR characterization.**

1. INTRODUCTION

Gold has been known to be catalytically inactive, however, it has recently been found (1, 2) that when dispersed as ultrafine particles Au exhibits an extraordinary high activity in many reactions, in particular in CO oxidation at low temperatures. The activity of gold supported on TiO_2 strongly depends on the size of Au particles: the rate of the CO oxidation reaction markedly increases with a decrease in the diameter of the Au particles. It has been hypothesized that CO is oxidized at the perimeter interface between gold and the support surface (3).

Recently, Goodman's group (4, 5) studied the oxidation of CO over model catalysts prepared in UHV conditions and found a strong dependence of the CO oxidation activity on the Au cluster size. They proposed, on the basis of scanning tunneling microscopy/spectroscopy (STM/STS) results, that the structure sensitivity of this reaction on Au/TiO_2 can be related to the thickness of the gold islands. In particular, they found that islands of two or three atom layers thick are the most effective for catalyzing the oxidation of CO, more than three-dimensional (3D) particles. In addition to these structural parameters, it was shown by STS that the 2D clusters and the two or three atomic layer thick clusters tend to lose metallic character with a band gap of 0.8–0.3 V. They correlated the catalytic properties to unusual electronic properties of the gold particles with a thickness of 2–3 atomic layers. Mavrikakis *et al.* (6) investigated very recently the question of the dependence of the reactivity of gold on the particle size on the basis of self-consistent density functional calculations. They studied the adsorption of O atoms and CO on flat and stepped Au(111) slabs with one to six layers and also on Au(211) slabs. They found that there is little variation in the chemical activity of Au(111) with the slab thickness except for the one layer slab, which is substantially less reactive than the thicker slabs. Steps were found to bind the adsorbates stronger than the (111) terraces. In a combined variable temperature STM-HREELS study (7) it was shown that Au edge atoms on Au layers deposited on Pd(111) substrate are sites of a strongly enhanced Au–CO interaction compared with CO adsorption on Au terraces. This fact is attributed to a modification in the electronic properties of Au edge atoms related to their reduced coordination number. It was suggested that the unusually large catalytic activity of the highly dispersed Au particles may be in part due to the high step densities of the small particles and/or to strain effects due to the mismatch at the gold–titania interface.

[1] To whom correspondence should be addressed. E-mail: Boccuzzi@ch.unito.it.

0021-9517/01 $35.00

Up to now, the origin of the different catalytic properties of the same metal supported on different oxides appears not fully clarified, in particular it is not completely clear to which of the following effects the differences can be related: simply to the concentration of special, uncoordinated surface sites or to an electronic and chemical modification of the very small metallic particles by the supports or to structural modifications related to the strain of the very small particles in interaction with the support.

Although it is virtually impossible to prepare a collection of metallic particles that are truly monodispersed, i.e., having exactly the same size, in the past years significant progress occurred in the preparation of gold particles with a very narrow size distribution (8), by deposition of gold on the support at a fixed pH, followed by calcination in air at different temperatures. In this paper, we will present the catalytic data on three Au/TiO_2 samples with the same gold loading, but calcined at three different temperatures. The data will be discussed in relation to the size of the metallic particles determined by TEM and to FTIR results on CO adsorption and oxidation from 90 up to 300 K.

2. EXPERIMENTAL

Three Au/TiO_2 samples with the same actual Au loading, 1 wt%, were prepared by the deposition–precipitation method (9) at pH 7 and at 343 K, followed by calcination at 473, 573, and 873 K. Titanium dioxide, produced by Degussa (p-25, mainly composed of anatase, specific surface area 45 m^2/g), was used as support. Each sample will be labeled by its calcination temperature. Before the spectroscopic experiments, the samples were submitted to pretreatments that will be illustrated in the following.

Spectra were recorded on 1760 and 2000 Perkin–Elmer FTIR spectrometers (2 cm^{-1} resolution, 60 scans in normal conditions, 4 for spectra taken every 15 s), in which the samples in cells were allowed to run the spectra in controlled atmospheres and at different temperatures in the 90–300 K range. The catalytic experiments were carried out by using a fixed bed flow reactor. Reactant gas containing 1 vol% of CO or H_2 in air were passed through a 100-mg catalyst bed at a flow rate of 33 ml/min.

TEM observation was performed with a Hitachi H-9000NA electron microscope at an accelerating voltage of 300 kV. The samples were supported on copper mesh with carbon micro-grid. All TEM photographs were taken at a magnification of 200,000. TEM images were digitally processed from the negative films by using a film scanner. The mean diameters, standard deviations, and size distribution measurements of the gold particles were performed on digital images by using the image analyzing software, Image-Pro.

3. RESULTS AND DISCUSSION

3.1. Catalytic Activity

Figure 1 shows conversion vs temperature for CO oxidation on the three samples in comparison with that for H_2 oxidation. Over all three samples the conversion of CO oxidation reaches 100% at temperatures significantly lower than that of H_2 oxidation. This behavior implies that the CO molecule is more effectively activated on the Au surface than the H_2 molecule, which can react with oxygen molecules or atoms more readily when dissociated into atomic species. There is a large difference between the temperatures of 50% conversion in both the CO and the H_2 oxidation on the 473 and 573 K samples and those observed on the 873 K sample, while a similar gap in temperature between CO and H_2 oxidation is observed on all the samples. These features clearly indicate that the size of gold particles imposes an effect on both the oxidation reactions. Looking at the data of CO conversion, it appears evident that in the 230–250 K temperature range the 473 sample is significantly less active than sample 573. In contrast, almost no difference or an opposite difference is observed in the H_2 oxidation.

3.2. TEM Characterization

Figure 2 shows TEM images of the three calcined samples, (a) 473, (b) 573, and (c) 873 K. Gold particles are seen as dark contrasts on the surface of TiO_2 particles. The size distributions of Au particles for the above samples are shown in Figs. 3a–3c, respectively. The mean diameter is almost the same for the 473 and the 573 K samples; however, the fraction of particles of 1–2 nm apparently decreases with

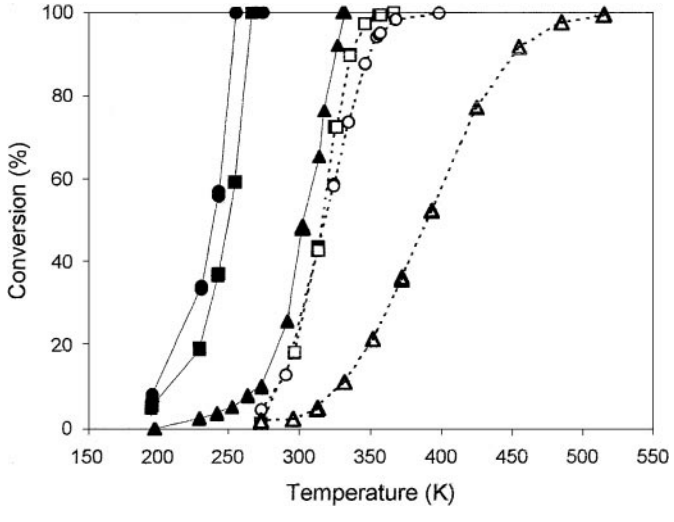

FIG. 1. Conversion vs temperature relation in the oxidation of CO (solid line, dark symbols) and H_2 (dotted line, open symbols) over Au/TiO_2 catalysts calcined at (□/■) 473, (○/●) 573, and (△/▲) 873 K.

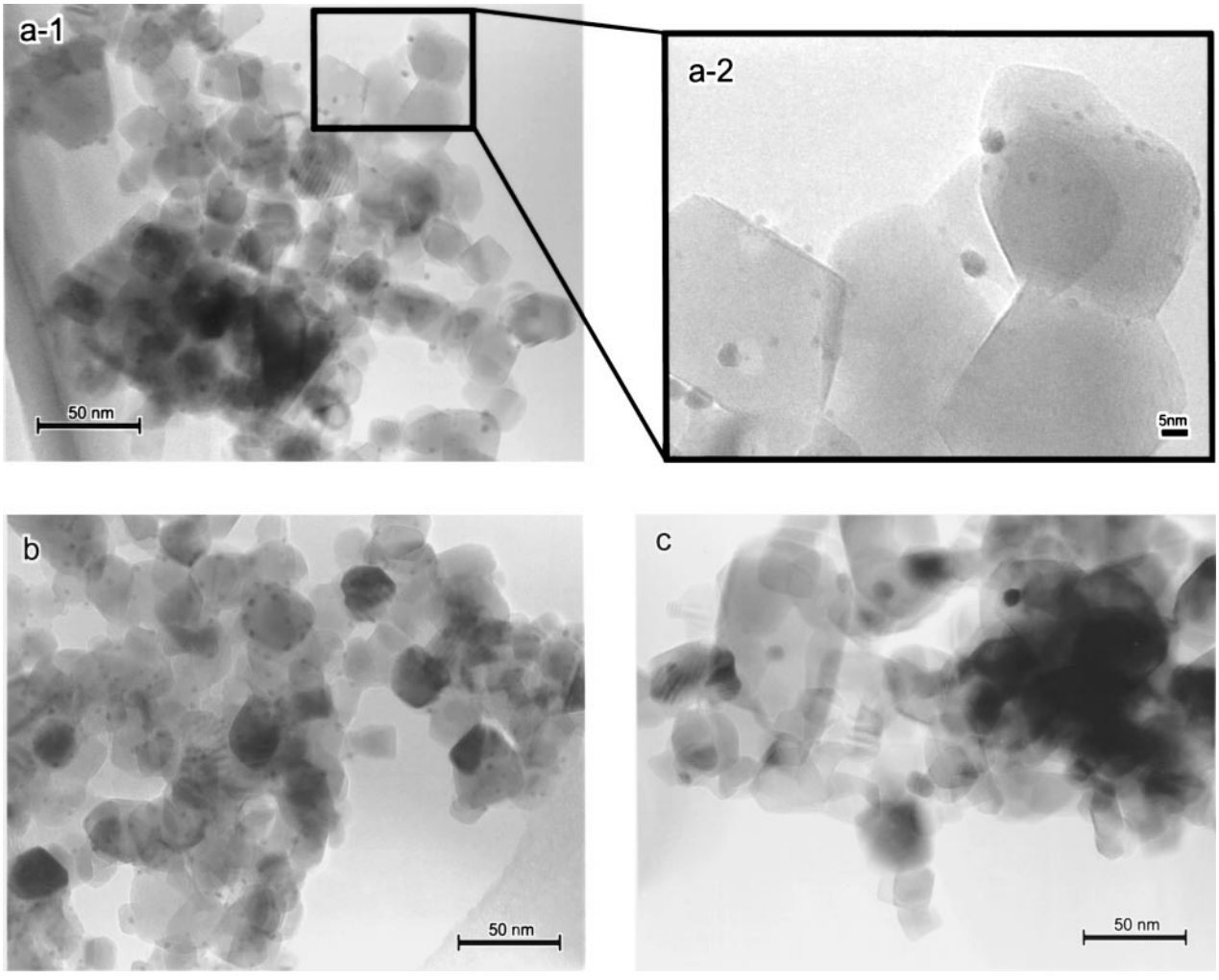

FIG. 2. TEM images of Au/TiO_2 catalysts calcined at (a) 473, (b) 573, and (c) 873 K taken at a magnification of 200,000. Partially enlarged image of section a is shown in the inset.

the increase in calcination temperature. This suggests that the large particles are formed after calcination by coagulation of small particles.

Gold particles on the 873 K sample are much larger and show a much broader size distribution, as shown in Fig. 3c. Mean diameter and size distribution apparently shift to larger values from 573 to 873 K. No particles with diameter below 4 nm were seen after calcination at this temperature.

3.3. FTIR Measurements at 90 K

3.3.1. FTIR spectra of CO adsorbed at 90 K on the three samples calcined in air. Figure 4a shows the FTIR spectra of CO adsorption on the three samples calcined in air at 473, 573, and 873 K. The samples were simply outgassed at room temperature, and the spectra were obtained after interaction with 4 mbar of CO at 90 K, normalized on the intensity of the absorption band at 2150 cm^{-1}. This band, assigned to CO interaction by hydrogen bond with the surface OH groups, can be taken as a measure of the exposed hydroxylated titania area. In fact, by outgassing at 90 K the band is completely depleted and at the same time the strong perturbation observed in the OH stretching region of the titania hydroxyls almost completely disappears. Some small differences will be discussed and illustrated later on. The normalization leads to very similar spectra in the OH stretching and in water bending regions (not shown for the sake of brevity). Similar relative intensities were obtained also normalizing the spectra on the intensity of the pellet absorption at 1050 cm^{-1}, on the vibrational edge of TiO_2.

It is clear that the band at about 2100 cm^{-1} is completely absent in the 873 K sample and it is stronger on the 573 K than on the 473 K sample. The absorption at 2100 cm^{-1}, according to our previous data and the literature (10, 11), is assigned to CO chemisorbed on metallic gold sites. The 873 K sample is characterized by metallic particles a little larger than 10 nm and, by assuming an ideal Wulff geometry (12), with a ratio of edge Au atoms to total Au atoms < 0.1. The

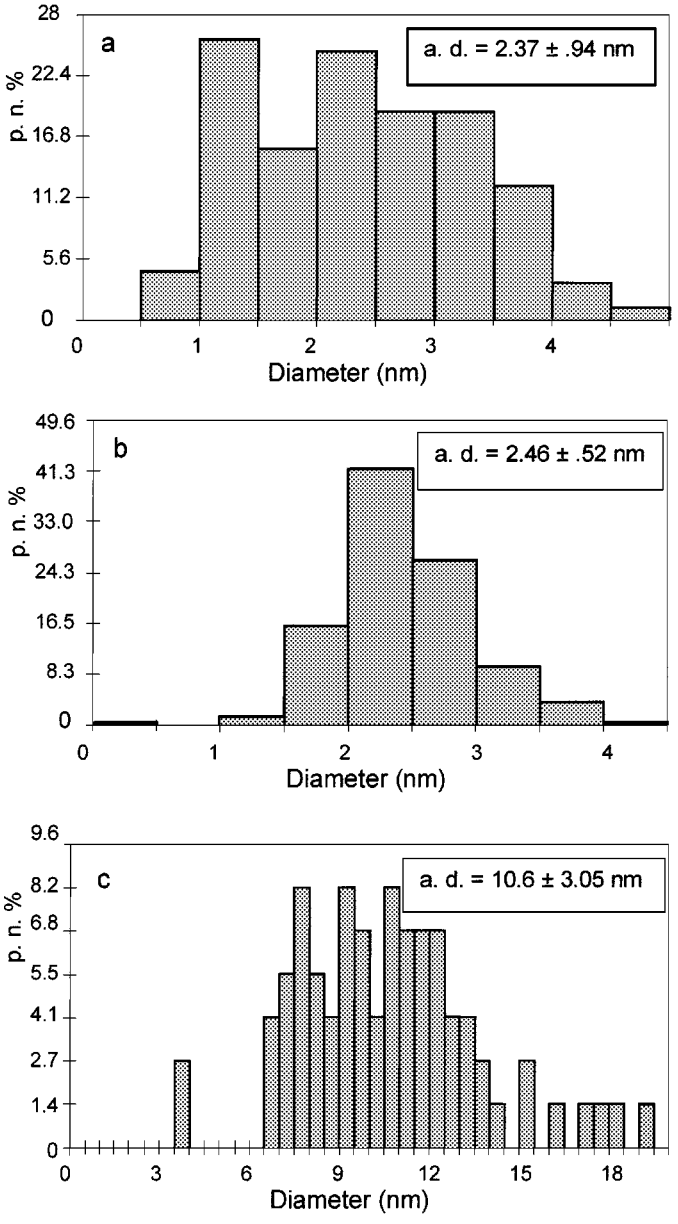

FIG. 3. Size distributions of Au particles for the samples 473, 573, and 873 K shown in the micrographs of Fig. 2. The average diameters are reported in the labels.

complete absence on this sample of the band at 2100 cm^{-1} strongly indicates that even at a temperature as low as 90 K *only the step sites* are able to adsorb CO, while gold terrace sites, which constitute the large majority of the exposed gold sites, do not adsorb CO at all at 90 K. These results are in good agreement with the adsorption energy of CO determined by GGA self-consistent density functional calculations as for the Au(111) and the Au(211) surfaces (6).

As for the 2176 cm^{-1} band the frequency region is typical of CO adsorption on cationic sites. Its frequency and intensity are almost identical on the three samples and does not shift by reducing the CO pressure. Different hypotheses can be proposed for the assignment of this band: (i) CO adsorbed on Ti^{4+} ions; (ii) CO on cationic gold, and (iii) CO on isolated gold atoms bonded to a peroxo species. The first hypothesis can be ruled out because the surfaces are simply outgassed at room temperature, so that they are completely hydrated and hydroxylated and therefore they do not expose coordinatively unsaturated Ti^{4+} ions. The spectra of CO adsorbed at 77 K on pure Degussa p-25 exhibited a strong, complex absorption in this region only after activation and dehydration at 873 K, whose frequency blue-shifts by decreasing coverage (13). Other hypotheses, i.e., CO adsorbed on cationic gold sites possibly at the contact line between the metallic particles and the support or on isolated gold atoms bonded to a peroxo species, can be proposed. A band at around 2175 cm^{-1}, assigned to CO on cationic Au sites, is reported on Au/SiO_2 samples (14). In the scheme reported in the last review of Bond and Thompson (15), cationic gold sites at the interface between the support and the gold particle, acting as a chemical glue, are reported. However, it can be noticed that the intensity of the 2176 cm^{-1} band is almost the same in the three samples; therefore, this hypothesis does not appear very likely. Huber *et al.* (16) reported that, by cocondensation at 10 K

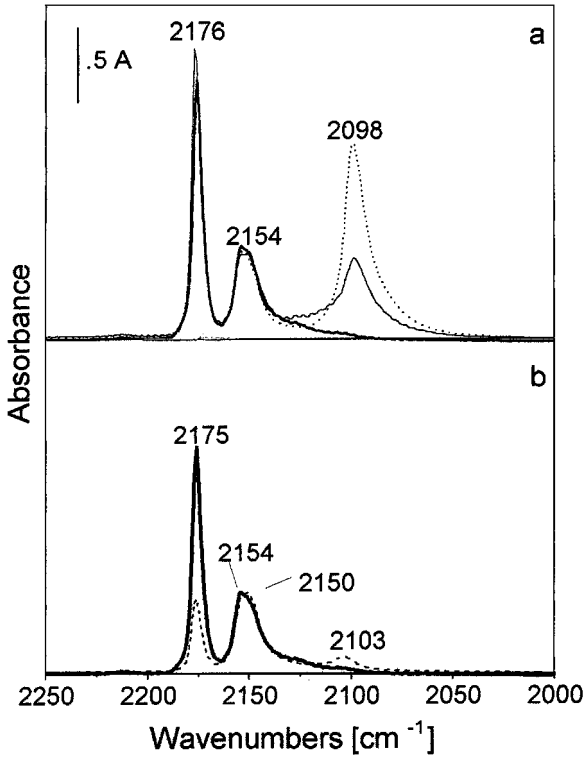

FIG. 4. FTIR absorbance spectra of CO adsorbed at 90 K in the carbonylic region: (a) 4 mbar of CO adsorbed on (fine line) sample calcined at 473 K, (dashed line) calcined at 573 K, (bold line) calcined at 873 K; (b) FTIR absorbance spectra of 4 mbar of CO adsorbed at 90 K on (bold line) calcined at 873 K, (dashed line) readmission of CO on the same sample at RT and cooled to 90 K.

in matrix of Au atoms with CO and oxygen, an unstable and reactive species was formed, characterized by a band at 2176 cm^{-1}, assigned to the CO stretching of a monoatomic carbonyl peroxo Au species. The comparison of the spectrum produced by the inlet of 4 mbar of CO at 90 K on a sample calcined at 873 K with the spectrum produced by the interaction with CO at room temperature on the same sample and by successive cooling to 90 K (Fig. 4b) shows that at the end of this procedure a weak 2100 cm^{-1} band appears and at the same time the intensity of a 2176 cm^{-1} peak is significantly reduced. It can be assumed that the interaction with CO up to room temperature results in the decomposition of isolated carbonyl peroxo species and to their agglomeration in metallic particles, able to give the 2100 cm^{-1} band.

As for the absorption band at 2100 cm^{-1}, its lower intensity on the 473 K sample than on the 573 K sample, in spite of a little smaller mean diameter of the metallic Au particles, can be explained by assuming that on the 473 K sample a significant fraction of Au at the end of the preparation is still not metallic but in an oxidized state. In the presence of oxygen, Au_2O_3 bulk phase is more stable than metallic Au up to 410 K (17). Highly dispersed phases may have higher stability than bulk phases. By interaction with CO at 90 K, these Au species remain in their oxidized form, unable to adsorb CO. The 573 K sample has been prepared at a temperature high enough to transform Au species into the metallic state at the end of the preparation and therefore shows higher intensity of the 2100 cm^{-1} band. This finding is in agreement with the analysis of the X-ray absorption fine structure (XAFS) and X-ray adsorption near edge structure (XANES) results (18) of samples prepared at the same temperatures.

Figures 5a and 5b illustrate the behavior of the absorption bands of the 473 and 573 K samples shown in Fig. 4a by decreasing the CO pressure from 4 mbar to 10^{-2} mbar at 90 K. The 2150 cm^{-1} band is completely depleted and the 2176 cm^{-1} band strongly reduces its intensity, while the 2100 cm^{-1} band shows an erosion from the low frequency side, producing a blue shift of the band up to 2102 cm^{-1}. Moreover, looking at the inset of Fig. 5b, it appears evident that at 90 K a component centered at 2098 cm^{-1} is reversible to the outgassing. Different hypotheses can be made as for the assignment of the species related to the two components in the carbonylic region. It can be hypothesized that CO is adsorbed on two kinds of step sites: step sites on top of the particles for the 2102 cm^{-1} band and step sites close to the contact perimeter with the support for the 2098 cm^{-1} band. The red shift of the more labile band, the 2098 cm^{-1}, in respect to the irreversible band, the 2102 cm^{-1}, may be ascribed to an electric field acting on the borderline sites (19).

3.3.2. CO–O_2 interactions and reactions at 90 K on the samples calcined in air. In Figs. 6a and 6b, two different CO–O_2 interactions at 90 K are shown on the samples calcined at 473 and 573 K in air. No data are reported for the 873 K sample, because no significant effects on the CO absorption features were observed in this case by oxygen inlet. The admission of O_2 at 90 K (fine line) on preadsorbed CO (dotted line) on the 473 K sample (Fig. 6a) produces a very small blue shift of the 2098 cm^{-1} band without changes in the intensity, a small erosion of the absorption from the low frequency side, and a weak band at 2340 cm^{-1}. The weak band at 2340 cm^{-1} indicates the formation of CO_2, already at 90 K. The shift and the small erosion can be taken as an indication that molecular oxygen is activated and reacts with the CO species weakly adsorbed on step sites closer to the borderline with the support or modified by coadsorbed water or hydrogen.

The inlet of CO on preadsorbed oxygen produces a spectrum substantially different (bold line): the 2098 cm^{-1} band is almost completely depleted, no shifts or new bands are produced and the 2340 cm^{-1} band is absent. It appears, from these data, that *oxygen* and *CO* are competitively adsorbed at 90 K on the same gold sites.

The $^{18}O_2$ inlet at 90 K (Fig. 6b, fine line) on preadsorbed CO (dotted line) on the 573 K sample produces a large

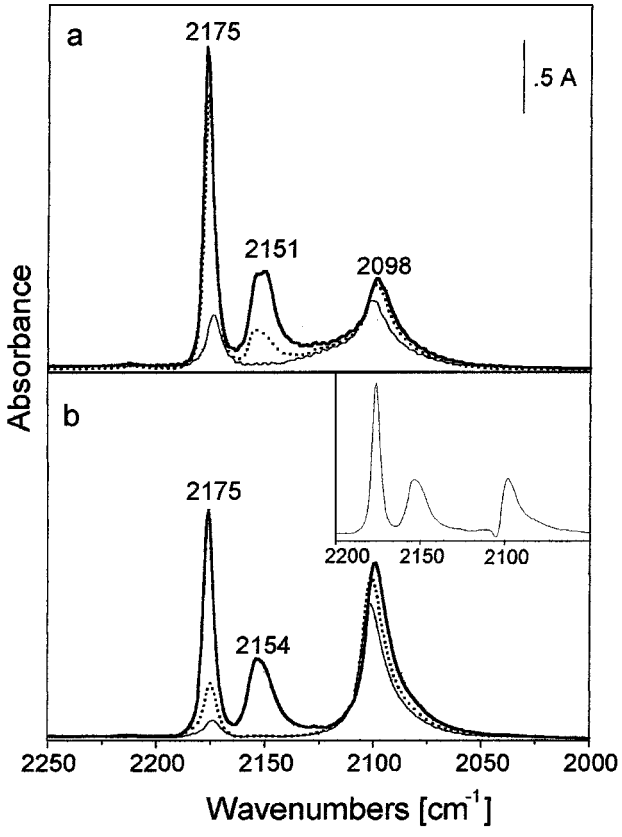

FIG. 5. Pressure dependence of the FTIR absorbance spectra of CO adsorbed at 90 K on the (a) 473 K and on the (b) 573 K samples: (bold line) 4 mbar of CO, (dotted line) 1 mbar of CO, (fine line) 0.01 mbar of CO. Inset in (b): difference spectrum in the 2200–2000 cm^{-1} range between bold and fine lines.

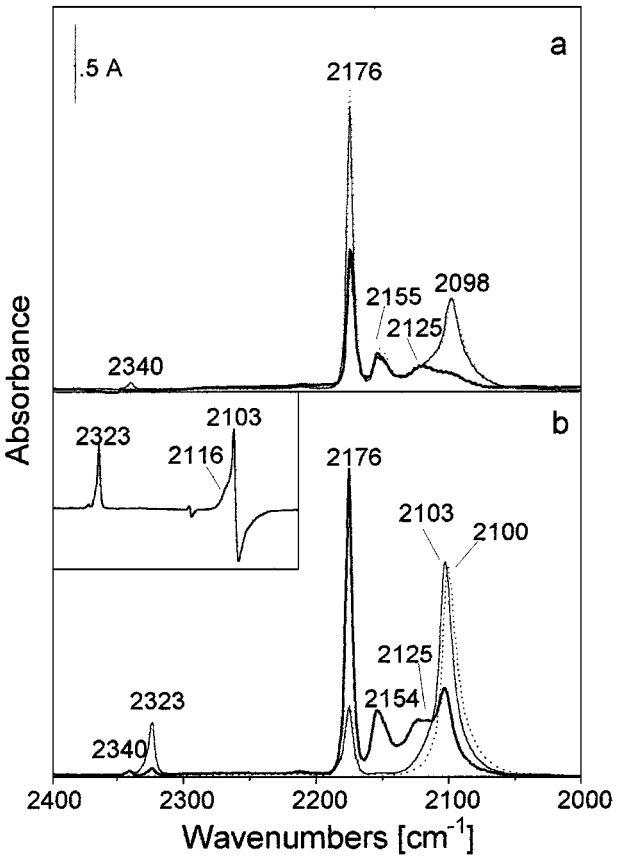

FIG. 6. FTIR absorbance spectra at 90 K of different CO–$^{16}O_2$ (on the 473 K, (a)) and CO–$^{18}O_2$ (on the 573 K, (b)) interactions; (dotted lines) 2 mbar of CO, (fine lines) 2 mbar of $^{16}O_2$ (or $^{18}O_2$) on preadsorbed CO, (bold lines) 2 mbar of CO on preadsorbed $^{16}O_2$ (or $^{18}O_2$). Inset in (b): difference spectrum between fine and dotted lines.

erosion from the low frequency side of the carbonylic band, its small blue shift, from 2100 up to 2103 cm^{-1}, and the growth of a shoulder at 2116 cm^{-1} (see inset). At the same time a band at 2323 cm^{-1} assigned to $C^{16}O^{18}O$ solid like grows up, accompanied by a very weak band at 2340 cm^{-1}, assigned to $C^{16}O_2$ solid like phase. The erosion of the band at 2099 cm^{-1} is similar to that produced by the decrease of CO pressure, reported in Fig. 4. The formation, almost exclusively, of $C^{16}O^{18}O$ indicates that the oxygen participating in the reaction at 90 K is mainly the oxygen coming from the gas phase. It can be suggested that *oxygen molecules* are in some way activated and dissociated on the sites where CO is reversibly adsorbed at 90 K. Some of the produced atomic oxygen may react with CO giving rise to the $C^{16}O^{18}O$ formation, other oxygen atoms may remain coadsorbed with CO on the step sites, producing the blue- shifted 2116-cm^{-1} component. Therefore, the band at 2116 cm^{-1} can be assigned to the CO–$Au_s^{\delta+}$–$O^{\delta-}$ surface species. In the case of oxygen preadsorption (Fig. 6b, bold line), CO adsorption on the metallic particles is in some extent inhibited (strong reduction of the intensity of the 2100 cm^{-1} band) and in part strongly modified (band at 2125 cm^{-1}). An electron transfer from the metal to the adsorbed oxygen molecules can explain this feature. We assign the 2125 cm^{-1} band to CO adsorbed on metallic gold sites interacting with a superoxidic or peroxidic oxygen molecular species:

$$O_2^{\delta-}\text{–}Au^{\delta+}\text{–}CO \quad \nu CO = 2125\,\text{cm}^{-1}.$$

The bands observed previously in the same spectral region on Cu/ZnO and on Cu/TiO_2 (20) and on Cu/SiO_2 (21) may have the same assignment. In fact, bands in the 2120–2140 cm^{-1} region were observed only by interaction with CO after molecular oxygen and not after interaction with molecules producing atomic oxygen, as N_2O and NO.

3.3.3. Moisture effects on the CO oxidation with $^{18}O_2$ at 90 K. In the previous section we have discussed the differences observed in two different CO–O_2 and O_2–CO interactions. Here we will discuss the effect of moisture added to CO in the gas phase on the catalyst precovered with $^{18}O_2$. The experiment has been performed in order to clarify the controversial effect of moisture on the CO oxidation on gold catalysts (22). Figure 7, bold line, shows the spectrum produced by the interaction of 0.5 mbar of wet CO ($H_2O : CO \cong 1 : 3$) on preadsorbed $^{18}O_2$ at 90 K on the 573 K sample, in comparison with the spectrum of the same interaction with dry CO (dotted curve) and with that of CO alone (fine line). The experiments were carried out on the same sample in sequence, in dry CO first, then in wet CO, simply after outgassing at RT. In the presence of moisture in the gas phase the band assigned to $C^{16}O^{18}O$ shows an intensity similar to that observed on the same sample by interaction of $^{18}O_2$ on preadsorbed CO (Fig. 6b, fine line).

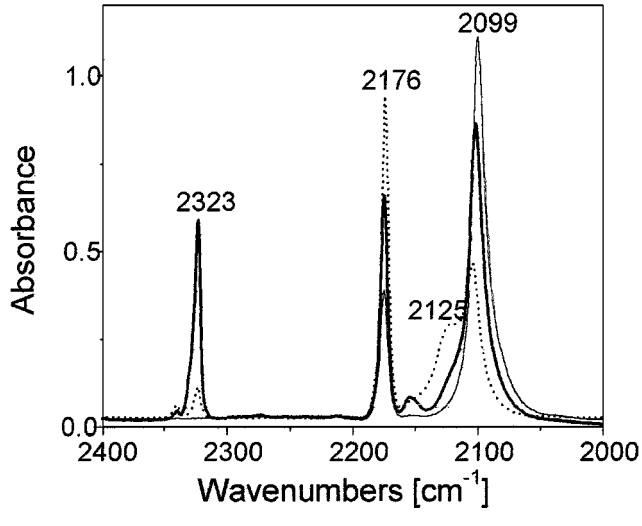

FIG. 7. FTIR absorbance spectra on 573 K sample at 90 K: (fine line) 0.5 mbar of pure CO, (bold line) 0.5 mbar of wet CO ($H_2O : CO \cong 1 : 3$) on preadsorbed $^{18}O_2$, (dotted curve) 0.5 mbar of dry CO on preadsorbed $^{18}O_2$.

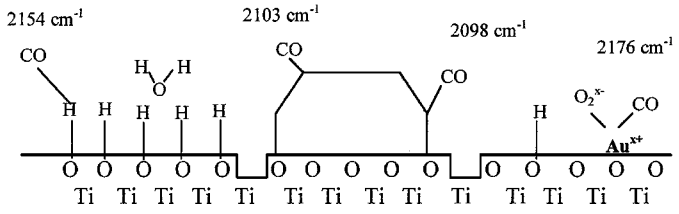

SCHEME 1. CO interactions at 90 K.

Also in this case only $C^{16}O^{18}O$ is formed in the reaction, without any participation of the oxygen of the support or of the water. The 2125 cm^{-1} band is strongly reduced and the 2099 cm^{-1} band shows an intensity similar to that observed in the absence of oxygen, only slightly lower. It has been already reported (10, 23) that CO and water interaction produces CO_2 and hydrogen when water is present in the gas phase on Au/TiO_2 catalyst at room temperature. An hypothesis could be that hydrogen atoms of the water present in the gas phase react with the *superoxo species* adsorbed on gold metallic sites, producing firstly a very unstable and reactive OOH^- species and then nascent oxygen and OH groups. The *nascent oxygen* can react with CO producing $C^{16}O^{18}O$.

From these experiments it appears evident that the reaction of water with CO can help the oxygen dissociation on the gold step sites, therefore explaining the promoting effect of water on the reaction. It should be noted that a positive effect of the moisture on the reaction is produced already at 90 K. As for the 2176 cm^{-1} band, assigned to a carbonyl gold peroxo species, its intensity increases in both the oxygen interactions, confirming the assignment previously proposed.

TABLE 1

Abundance of Different Au Sites as Revealed by CO Adsorption at 90 K

Sample	Metallic step sites (2103 cm^{-1}, irreversible)	Metallic corner sites or step sites on the borderline of the particles (2098 cm^{-1}, reversible)	Isolated carbonyl peroxo species (2176 cm^{-1})
473 K	few	many	some
573 K	many	many	some
873 K	very few	none	some

3.3.4. Adsorbed species and reaction mechanism of CO oxidation at 90 K. It has been proposed that CO is irreversibly adsorbed on step metallic gold sites, reversibly on corner sites exposed at the surface of the smallest particles and on borderline sites close to the support, possibly modified by coadsorbed species (water, H, OH), and also on gold atoms interacting with a peroxo species. The relative amounts of the species are different on the three samples.

Scheme 1 and Table 1 summarize the main features of CO adsorbed on Au/TiO_2 at 90 K. Scheme 2 shows the coadsorption of O_2 and CO and their reactive interaction.

If oxygen is preadsorbed at 90 K in the absence of gas phase moisture, the preadsorbed peroxo species is inactive

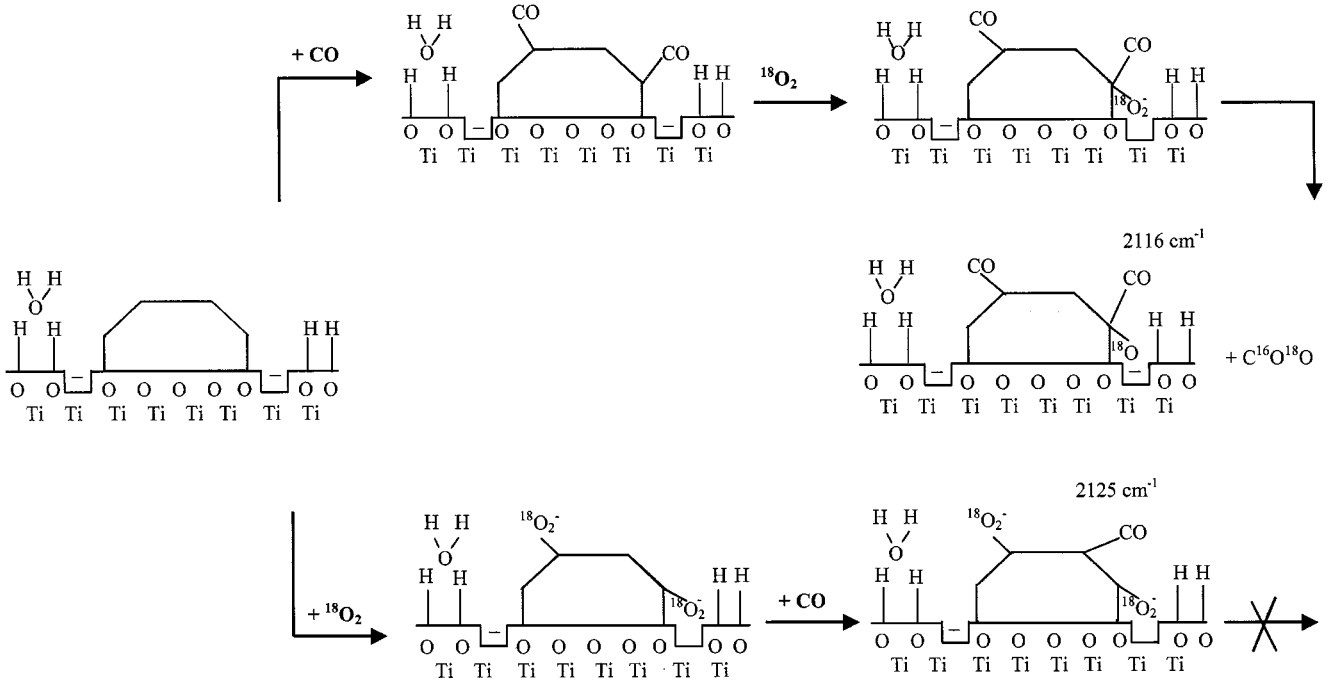

SCHEME 2. CO–O_2 interactions at 90 K.

in the CO oxidation at 90 K. As for the origin of the asymmetric behavior of the two CO–O_2 interactions (1) and (2) illustrated in Figs. 6a and 6b, it can be hypothesized that the asymmetry is generated by the intrinsic differences of the two ligands: CO acts as a two electron donor and oxygen as a one electron acceptor. CO preadsorbed, acting as a two electron donor (24, 25), can make an electron transfer from the gold to the oxygen easier and larger. Oxygen preadsorbed on the more uncoordinated exposed sites, the corner sites, inhibits CO adsorption and modifies vicinal step sites. On this basis it can be rationalized why on the 473 K sample, exhibiting in HRTEM analysis a large fraction of very small metallic particles, where no terrace and step sites are present but only corner sites, very weak CO bands are detected by inlet of CO after oxygen interaction.

Sanchez *et al.* (26) proposed different models for the CO oxidation on the basis of temperature-programmed reaction studies of CO oxidation and ab initio simulations for gold clusters supported on either a defect-free or defect-rich MgO. Among them, the Langmuir–Hinshelwood model (LH_p), where CO is adsorbed on the top facet of the gold cluster and the peroxo species is bonded at the perimeter between the cluster and the support, can be taken as a model for the behavior of the small gold particles supported on titania.

It can be relevant to observe that the temperature of CO combustion on gold clusters supported on defect-rich MgO, 240 K (26), is very close to the temperature of the rapid increase in the conversion of CO on the 473 and 573 K samples.

In conclusion, on gold catalysts at low temperatures the reaction occurs according to mechanism similar to that of Langmuir–Hinshelwood, generally accepted for the reaction on more traditional metallic catalysts (Pt, Pd, and Rh) at higher temperatures between adsorbed CO and adsorbed oxygen. However, some differences must be taken into account. Differently from the other metals, CO is weakly bonded on the Au surfaces and its preadsorption does not inhibit oxygen adsorption; moreover, while the other metals easily dissociate oxygen molecules already at low temperatures, clean gold step sites do not dissociate oxygen. Oxygen can be reactively activated in presence of CO on sites at the borderline of the metallic particles, probably at oxygen-vacancy defects, as reported in Scheme 2.

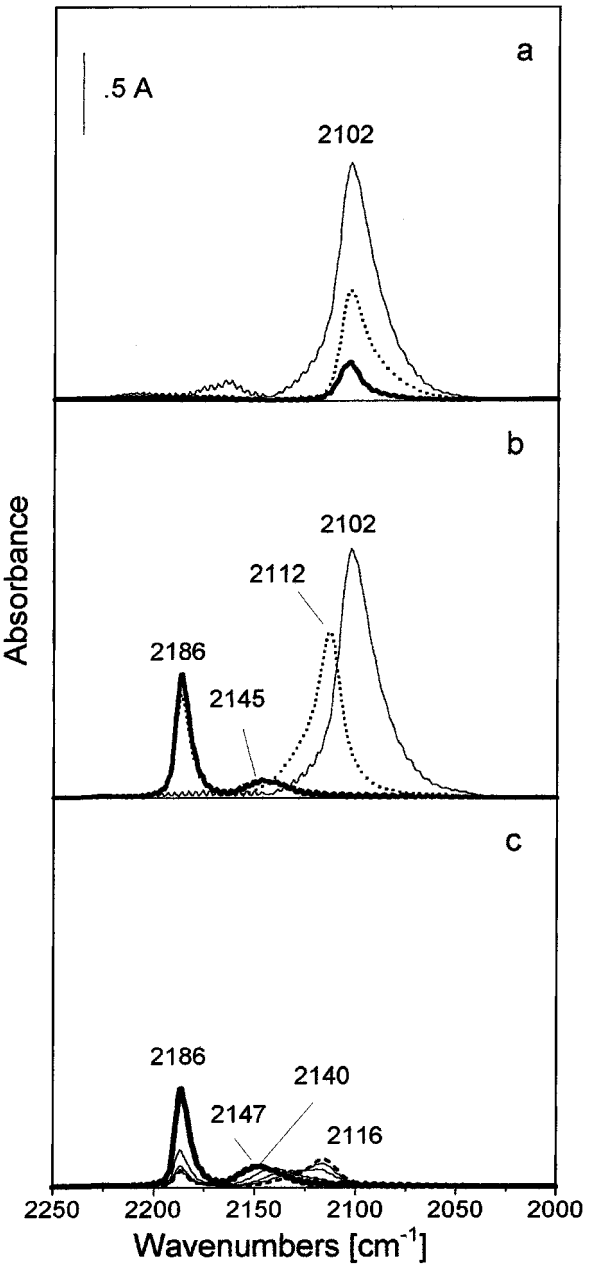

FIG. 8. FTIR absorbance spectra run at 300 K. (a and b) 10 mbar of CO on 473 K (fine lines), 573 K (dotted lines) and on 873 K (bold lines) calcined in air (a) and pretreated in the spectroscopic cell in dry oxygen (b). The spectra of the three samples have been normalized, as reported in the text. (c) Effect on the bold spectrum of (b) (10 mbar of CO on 873 K sample pretreated in the spectroscopic cell in dry oxygen) of the inlet of 10 mbar of hydrogen with the contact times (fine lines and dashed line).

3.4. FTIR Measurements at 300 K

3.4.1. FTIR spectra of CO adsorbed at 300 K on the three samples. Figure 8a shows the spectra produced by interaction with 10 mbar of CO at 300 K on the three samples calcined in air at 473, 573, and 873 K and simply outgassed at room temperature before interaction. The spectra were normalized on the basis of the bending intensity of the adsorbed water, taken as a measure of the exposed surface area. The band at 2103 cm^{-1} is strong and broad on the 473 K sample, weaker and narrower on the 573 K sample, and very weak on the 873 K sample. The differences from the spectra taken at 90 K, shown in Fig. 4a, are relevant: in particular the 2100 cm^{-1} band was completely absent in the 873 K sample and an inversion in the intensity of the 2100 cm^{-1} band is observed between the 473 and 573 K samples. As already stated in Section 3.3.1,

on the 473 K sample a significant fraction of gold is not metallic, but in a highly dispersed, oxidized state. By interaction with CO at 90 K we have shown that these gold species remain in their oxidized form, while by interaction with CO at 300 K these gold species are reduced by CO, giving rise to a strong and broad absorption band, due to CO adsorbed on amorphous, disordered sites of metallic Au. Similarly, the presence of a band at 2100 cm^{-1} on the 873 K sample at RT can be taken again as a confirmation that CO interaction reduces oxidized Au sites.

Looking at the spectra reported in Fig. 8b, taken on samples pretreated in dry oxygen at temperatures 50 K lower than their calcination temperatures and cooled down to RT in oxygen, strong differences are evident. On the 573 and 873 K samples a band at 2186 cm^{-1} is evident, due to CO interacting with Ti^{4+} exposed surface sites. This band is lacking on the 473 K sample, still fully hydrated. As for CO adsorbed on the metallic particles, a band at 2102 cm^{-1} strong, broad, and quite symmetric is observed on the 473 K sample, a weaker, narrower band, blue shifted to 2112 cm^{-1} and exhibiting a shoulder at 2130 cm^{-1} is observed on the 573 K sample, and a band still less strong and blue shifted to 2147 cm^{-1} is detected on the 873 K sample. As for the strong and broad band at 2102 cm^{-1} observed on the 473 K sample, in contrast to what is observed by interaction at low temperature, it can be proposed that CO is adsorbed on gold atoms in a disordered and amorphous-like phase, produced by the *in situ* reduction of an oxidized phase. A similar phenomenon was observed on Cu/ZnO samples very mildly reduced (27): CO adsorbed at the liquid nitrogen temperature revealed a weak band assigned to CO adsorbed on metallic copper particles and a band assigned to CO adsorbed on unreduced cationic copper, while after interaction on the same sample with CO at room temperature, a broader and stronger band was detected. The gold produced by *in situ* reduction by CO interaction can be in a liquid-like state: by TEM observation it was deduced, looking at the disappearance of the diffraction rings, that the 2-nm particles melt at about 573 K (28). In the XAFS spectra of Au/TiO_2 samples calcined at 473 K, a feature characteristic of oxidic gold is observed, which is almost completely absent in the samples calcined at 573 K (18). Similarly, the presence of a band at about 2100 cm^{-1} in Fig. 8a on the 873 K sample and the absence on the same sample in Fig. 8b can be taken as evidence that CO interaction at room temperature produced Au° sites by the reduction of oxidized sites.

As for the less strong and up-shifted band at 2147 cm^{-1} detected on the 873 K sample, evidence that this band can be related to CO adsorbed on gold step sites with coadsorbed molecular oxygen is given by the experiment illustrated in Fig. 8c. The inlet of molecular hydrogen at room temperature gradually reduces the intensity of the 2147 cm^{-1} band and produces a new component at 2116 cm^{-1}. At the same time absorption bands appear in the 3600–3200 cm^{-1} range and at 1610 cm^{-1} (not shown for sake of brevity) that can be assigned to the stretching and bending vibrational modes of water formed by reaction of hydrogen with oxygen. It can be therefore proposed that the 2147 cm^{-1} band is related to the CO coadsorbed with molecular oxygen on the few isolated step sites exposed at the surface of the larger and thicker gold particles characteristic of this sample. The surface species have the same structure already proposed for the assignment of the 2125 cm^{-1} band, $CO–Au_s^{\delta+}–O_2^{\delta-}$, the frequency is modified probably as a consequence of a different degree of charge transfer from gold to oxygen. On these sites hydrogen can be dissociated and it can react with the activated oxygen giving rise to water and adsorbed oxygen, possibly according to the reaction

$$CO–Au_s^{\delta+}–O_2^{\delta-} + H_2 \rightarrow \left[CO–Au_s^{\delta+}–HO_2^{\delta-}\right] + H \rightarrow CO–Au_s^{\delta+}O^{\delta-} + H_2O.$$

The band at 2116 cm^{-1} is assigned to the $CO–Au_s^{\delta+}–O^{\delta-}$ surface species, as we have already made, looking at the experiments illustrated in Fig. 6b. A band in the same spectral region was observed previously by some of us on supported copper catalysts (20). The lower frequency in respect to the other species can be explained by the higher electron affinity of molecular oxygen than atomic oxygen.

3.4.2. $CO–^{18}O_2$ and $CO–^{16}O_2$ interactions and reactions at 300 K on the samples pretreated in pure oxygen. Before the following experiments were run, all the samples were treated in oxygen in the IR cell, each one at a temperature 50 K lower than its calcination temperature, then they were cooled down to 300 K and finally outgassed.

After interaction of CO with preadsorbed $^{18}O_2$ at room temperature (Fig. 9, section a) on the 573 K sample, a triplet of absorption bands at 2351, 2334, and 2315 cm^{-1} assigned to $C^{16}O_2$, $C^{16}O^{18}O$, and $C^{18}O_2$ respectively, weakly adsorbed on titania, grows simultaneously in a short time (within 2 min). In the same time the intensity of the CO absorption band remains almost nihil. The intensity of the first two carbon dioxide components is similar, while the last component is weaker.

After 2 min the growth of the three bands stops and the intensity of CO absorption band grows up (Fig. 9b, dotted line). Moreover, a weak but definite band at about 2070 cm^{-1}, already assigned to the $C^{18}O$ stretching vibration, is also observed (full line).

Figure 9c, shows a comparison between $CO–^{16}O_2$ and $CO–^{18}O_2$ interactions at RT after 3 min of contact. As proposed by Liu *et al.* (29) the formation of doubly marked $C^{18}O^{18}O$, of $C^{16}O^{16}O$, and of $C^{18}O$ at room temperature is a consequence of secondary reactions, while $C^{16}O^{18}O$ is the primary product. The secondary products may be also produced by CO_2 readsorption in a labile and mobile

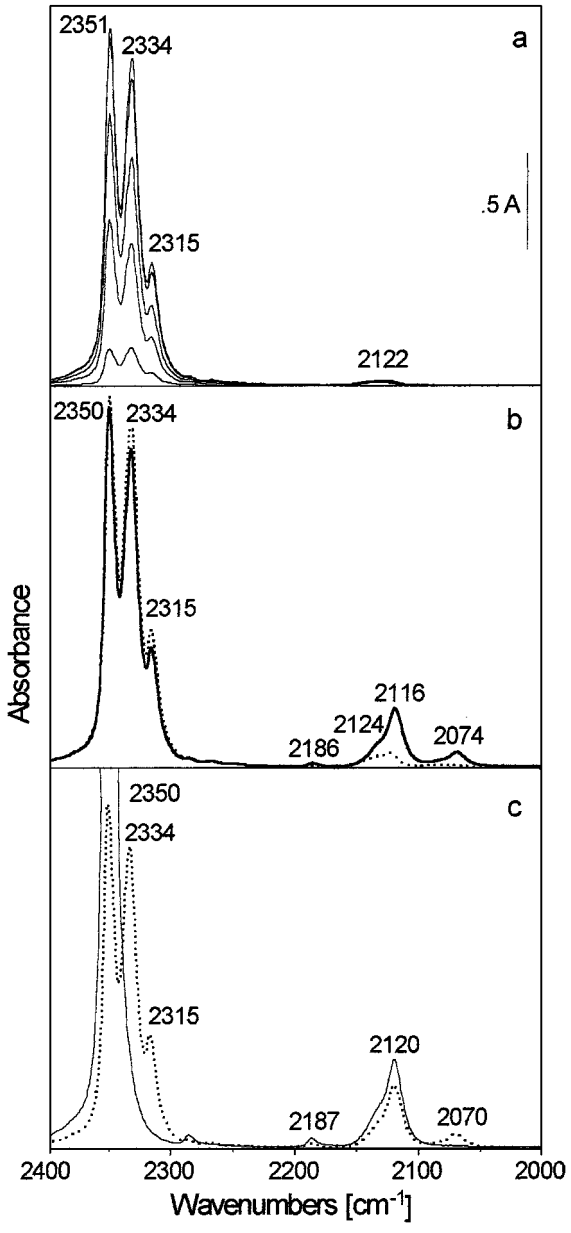

FIG. 9. FTIR absorbance spectra at 300 K of $^{18}O_2$–CO and $^{16}O_2$–CO reaction mixtures on the 573 K sample. (a and b) spectra run at different times during the diffusion of 10 mbar of CO on 5 mbar of preadsorbed $^{18}O_2$, every 15 s in (a), and after 2 min (dotted line) and 3 min (full line) of interaction in (b). (c) (dotted line) $^{18}O_2$–CO mixture, (full line) $^{16}O_2$–CO mixture, after 3 min of interaction.

molecular form on the support. Carbonate-like species are not involved in these reactions, as indicated by the absence of any change in their frequency and intensity by inlet of $^{18}O_2$, and therefore the carbonate-like species region, already shown in a previous paper, is not reported here (10).

Figure 10 shows the effect of oxygen interaction on preadsorbed CO at RT on the three samples. On the 473 K sample (Fig. 10a) the oxygen interaction produces a very strong decrease in the intensity of CO absorption band at 2102 cm^{-1}, assigned to CO chemisorbed on metallic Au produced in the in situ reduction of oxidic Au species. On the 573 K sample (Fig. 10b), the oxygen inlet produces only a small decrease and blue shift of the 2112 cm^{-1} band, assigned to CO chemisorbed on the steps of small metallic Au particles, a significant decrease of the band at 2186 cm^{-1} and a strong band at 2348 cm^{-1}. Finally, on the 873 K sample (Fig. 10c) the oxygen inlet produces no changes to the 2146 cm^{-1} band, assigned to surface species CO–$Au_s^{\delta+}$–$O_2^{\delta-}$, a significant decrease of the band at 2186 cm^{-1} assigned to CO

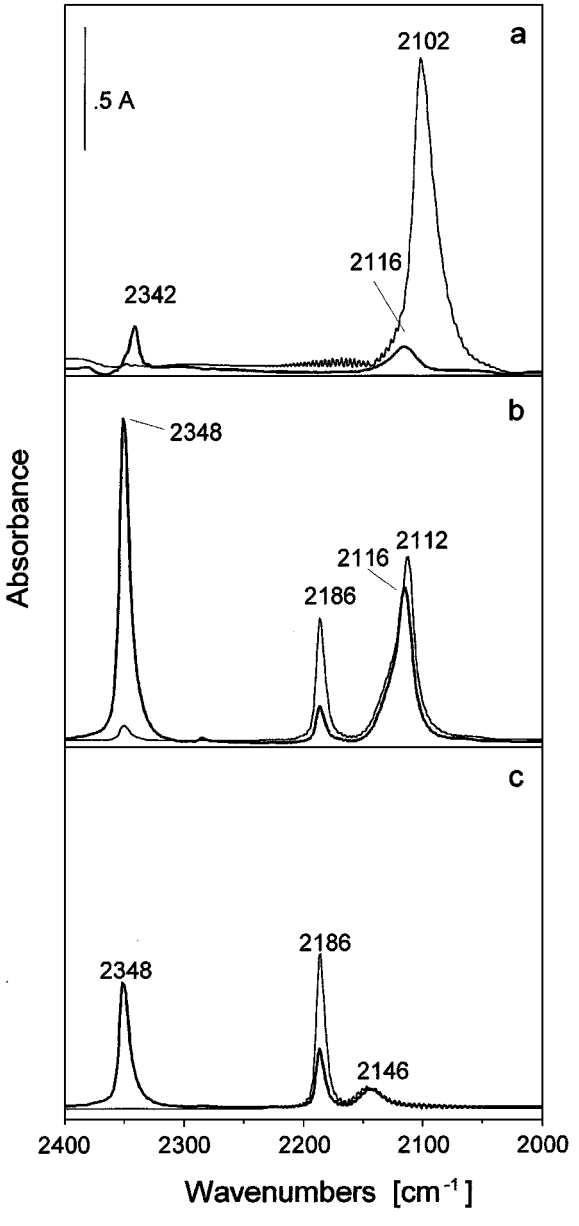

FIG. 10. FTIR absorbance spectra at 300 K of CO–$^{16}O_2$ reaction mixtures on (a) 473, (b) 573, and on (c) 873 K: (fine lines)10 mbar of pure CO, (bold lines) inlet of 5 mbar of O_2, spectra run after 15 min from the inlet of oxygen.

adsorbed on the support sites and a quite strong band at 2348 cm^{-1}.

From these experimental data it appears evident that at room temperature the activity of the catalysts is no more directly related to the free gold step sites available, as at low temperature. As shown by the experiments illustrated in the previous section, the mobility of the adsorbed species on the metallic particles and on the support and their exchange reaction play a significant role. In fact the catalytic data show a 100% conversion on all the samples.

As for the differences in the spectra between the 473 K and 573 K samples, Au atoms in a disordered, amorphous-like, thin layer have been produced by the *in situ* reduction of the oxidized phase on the 473 K sample. These gold sites may have a chemical behavior similar to that shown by Bondzie *et al.* (30) for *ultrathin gold particles*. It was shown that these gold sites were able to dissociatively adsorb O_2 more readily than thick gold particles; however, on these sites the rate of the reaction of CO with adsorbed oxygen is lower than on the thicker particles as a consequence of the stronger Au–O bond. These factors can explain the strong decrease, by oxygen inlet, of the band at 2102 cm^{-1} on the 473 K sample and, at the same time, the weak band at 2342 cm^{-1}, assigned to CO_2 weakly interacting with the support cations. The decrease in the intensity of the band assigned to CO interacting with Ti^{4+} sites is related to the reduction of the CO partial pressure in the cell.

3.4.3. Adsorption sites and mechanism of CO oxidation at 300 K. The presence of a multiplet of bands in the CO_2 stretching region after interaction with $^{18}O_2$, unlike at low temperature, clearly shows that the strong increase in the reaction rate at room temperature is mainly due to the participation of oxygen activated on the support: in CO oxidation in fact, an extensive exchange reaction with the oxygen atoms of the support occurs, as evidenced by the absorption bands related to the different CO_2 isotopomers. Moreover, by oxygen preadsorption on the 573 K sample, no competition or inhibition effects of oxygen on the CO oxidation have been put in evidence: in contrast, unlike at low temperature, before the growth of adsorbed CO bands, very strong CO_2 bands are detected in the first two minutes. The formation of doubly marked $C^{18}O^{18}O$, of $C^{16}O^{16}O$ and of $C^{18}O$, not observed in the low temperature experiments, could also be the consequence of secondary reactions, i.e. the CO_2 readsorption in a labile and mobile molecular form on the support, that can exchange oxygen atoms with the oxide. Anyway, carbonate-like species are not involved in these reactions: as already shown in a previous paper (10), the bands produced in the carbonate-like region during the CO–$^{16}O_2$ and CO–$^{18}O_2$ interactions are the same.

It can be proposed that at room temperature, the first step of the reaction is the adsorption of a mobile, molecular oxygen species on the support, followed by its dissociation, probably at the interface between the oxide and the metallic step sites, and a spill-over of O_{ad} to the Au particles, where finally the reaction takes place with the incoming CO.

CONCLUSIONS

Au/TiO_2 catalysts prepared by deposition–precipitation followed by calcination at 473, 573, and 873 K have mean diameters of Au particles of 2.4, 2.5, and 10.6 nm, respectively. The first two catalysts exhibit 100% conversion of CO at temperatures below 240 K, whereas the third catalyst exhibits 100% conversion at temperatures above 300 K. Moreover, FTIR data at 90 K show that this sample, that exposes in large majority gold terrace sites, does not adsorb CO at all.

Two kinds of gold step sites able to adsorb CO have been evidenced on the other two samples, step sites where CO is irreversibly adsorbed at 90 K and step sites where CO is reversibly adsorbed, probably *at the borderline* with the support. CO and O_2 are molecularly and competitively adsorbed on gold step sites, however there is evidence that CO preadsorption allows the reaction with O_2 to form CO_2, while oxygen preadsorption completely inhibits the reaction in the absence of moisture. The reaction in the presence of moisture at 90 K with $^{18}O_2$ produces only $C^{16}O^{18}O$.

The conclusions that can be drawn are: by CO preadsorption oxygen can be activated on gold step sites, close to the support and possibly to oxygen vacancies; by oxygen preadsorption and in the presence of moisture the reaction occurs probably because the superoxo species can react with the water coming from the gas phase producing nascent oxygen and OH groups; there is no direct participation of the oxygen of the support and of water in the reaction.

Finally, at room temperature other reaction channels must be operative, as revealed by participation of oxygen species activated on the support, shown by the extensive exchange reactions occurring with the support oxygen.

REFERENCES

1. Haruta, M., *Catal. Today* **36**, 153 (1997) and references therein.
2. Bond, G. C., and Thompson, D. T., *Catal. Rev. Sci. Eng.* **41**, 319 (1999) and references therein.
3. Haruta, M., Tsubota, S., Kogeyama, H., Genet, M., and Delmon, B., *J. Catal.* **144**, 175 (1993).
4. Valden, M., Pak, S., Lai, X., and Goodman, D. W., *Catal. Lett.* **56**, 7 (1998).
5. Valden, M., Lai, X., and Goodman, D. W., *Science* **281**, 1647 (1998).
6. Mavrikakis, M., Stoltze, P., and Norskov, J. K., *Catal. Lett.* **64**, 101 (2000).
7. Ruff, M., Frey, S., Gleich, B., and Behm, R. J., *Appl. Phys. A* **66**, S513 (1998).
8. Tsubota, S., Cunningham, D. A. H., Bando, Y., and Haruta, M., *in* "Preparation of Catalysts VI" (G. Poncelet, J. Martens, B. Delmon, P. A. Jacobs, and P. Grange, Eds.), pp. 227–235. Elsevier, Amsterdam, 1995.
9. Sakurai, M., Tsubota, S., and Haruta, M., *Appl. Catal. A* **102**, 125 (1993).

10. Boccuzzi, F., Chiorino, A., Tsubota, S., and Haruta, M., *J. Phys. Chem.* **100**, 3625 (1996).
11. Grunwaldt, J. D., and Baiker, A., *J. Phys. Chem. B.* **103**, 1002 (1999).
12. Wulff, G., Z. *Kristallogr.* **34**, 449 (1901).
13. Cerrato, G., Marchese, L., and Morterra C., *Appl. Surf. Sci.* **70/71**, 200 (1993).
14. Galvagno, S., and Parravano, G., *J. Catal.* **55**, 178 (1978).
15. Bond, G. C., and Thompson, D. T., *Gold Bull.* **33**, 41 (2000).
16. Huber, H., McIntosh, D., and Ozin, G. A., *Inorg. Chem.* **16**, 975 (1977).
17. Cotton, F., and Wilkinson, G., "Advanced Inorganic Chemistry" 3rd ed., p. 994. Wiley, New York, 1972.
18. Kageyama, H., Tsubota, S., Kadono, K., Fukumi, K., Akai, T., Kamijo, N., and Haruta, M., *J. Phys. IV France* **7**, C2 935(1997).
19. Liao, M. S., and Zhang Q. E., *J. Chem. Soc., Faraday Trans.* **94**, 1301 (1998).
20. Boccuzzi, F., and Chiorino, A., *J. Phys. Chem.* **100**, 3617 (1996).
21. Boccuzzi, F., Coluccia, S., Martra, G., and Ravasio, N., *J. Catal.* **184**, 316 (1999).
22. Bond G. C., and Thompson, D. T., *Gold Bull.* **33**, 41 (2000) and references therein.
23. Boccuzzi, F., Chiorino, A., Manzoli, M., Andreeva, D., and Tabakova, T., *J. Catal.* **188**, 176 (1999).
24. Wallace, W. T., and Whetten, R. L., *J. Phys. Chem. B* **104**, 10964 (2000).
25. Salisbury, B. E., Wallace, W. T., and Whetten, R. L., *Chem. Phys.* **262**, 119 (2000).
26. Sanchez, A., Abbet, S., Heiz, U., Schneider, W. D., Hakkinen, H., Barnett, R. N., and Landman, U., *J. Phys. Chem. A* **103**, 9573 (1999).
27. Ghiotti, G., and Boccuzzi, F., *Catal. Rev. Sci. Eng.* **29**, 151 (1987).
28. Buffat, Ph., and Borel, J. P., *Phys. Rev. A.* **13**, 2287 (1976).
29. Liu, H., Kozlov, A. I., Kozlova, A. P., Shido, T., Asakura, K., and Iwasawa, Y., *J. Catal.* **185**, 252 (1999).
30. Bondzie, V. A., Parker, S. C., and Campbell, C. T., *Catal. Lett.* **63**, 143 (1999).